Hindawi Publishing Corporation
Journal of Chemistry
Volume 2016, Article ID 6731848, 13 pages
http://dx.doi.org/10.1155/2016/6731848

Research Article

Numerical Simulation and Optimization of Enhanced Oil Recovery by the In Situ Generated CO_2 Huff-n-Puff Process with Compound Surfactant

Yong Tang,[1] Zhengyuan Su,[1] Jibo He,[1] and Fulin Yang[2]

[1]*The State Key Laboratory of Oil & Gas Reservoir Geology and Exploitation Engineering, Southwest Petroleum University, Chengdu 610500, China*
[2]*The Institute of Petroleum Engineering Technology, Jiangsu Oilfield Corporation, Yangzhou, Jiangsu 225009, China*

Correspondence should be addressed to Yong Tang; tangyong2004@126.com

Received 2 April 2016; Accepted 23 June 2016

Academic Editor: Jean-Luc Blin

This paper presents the numerical investigation and optimization of the operating parameters of the in situ generated CO_2 Huff-n-Puff method with compound surfactant on the performance of enhanced oil recovery. First, we conducted experiments of in situ generated CO_2 and surfactant flooding. Next, we constructed a single-well radial 3D numerical model using a thermal recovery chemical flooding simulator to simulate the process of CO_2 Huff-n-Puff. The activation energy and reaction enthalpy were calculated based on the reaction kinetics and thermodynamic models. The interpolation parameters were determined through history matching a series of surfactant core flooding results with the simulation model. The effect of compound surfactant on the Huff-n-Puff CO_2 process was demonstrated via a series of sensitivity studies to quantify the effects of a number of operation parameters including the injection volume and mole concentration of the reagent, the injection rate, the well shut-in time, and the oil withdrawal rate. Based on the daily production rate during the period of Huff-n-Puff, a desirable agreement was shown between the field applications and simulated results.

1. Introduction

Enhanced oil recovery (EOR) is the practice of implementing different techniques to increase crude oil production from a reservoir. According to the literature, the most commonly applied EOR techniques include thermal recovery, chemical injection, and gas injection. In the Permian Basin, CO_2 EOR and thermal methods continue to be the most dominant EOR field applications [1]. Furthermore, most oil fields are operated under water flooding.

It is well known that some oil will remain unproduced after water flooding (termed residual oil). Even though polymer flooding may reduce residual oil saturation, a significant portion of the oil will remain in the reservoirs. Surfactants then have to be injected to produce the residual oil [2]. Because acid and exothermic chemical reactions relieve deep reservoir damage, surfactants reach places in the formation where many polymers cannot enter, the injected surfactant decreases interfacial tension in oil-water contact, and CO_2 dissolved in oil increases oil volume that subsequently affects the displacement of residual oil [3]. Surfactant EOR is a fundamental method for the recovery of this residual oil. A number of factors impact the selection of the EOR technique and the resultant crude oil recovery. Generally speaking, these factors include the consideration of both technological availability and economic feasibility. Bera and Babadagli [4] tested foamy oil flow for different types of EOR gases dissolved and evolved at different conditions under pressure depletion. Their results showed that, among the three gases of CH_4, C_3H_8, and CO_2, CO_2 is a good candidate for foamy oil. Maximum oil recovery (more than 50% of the original oil in place [OOIP]) was obtained in the case of CO_2. Olsen [5] compared CO_2 flooding with water flooding. The test results showed that water flooding left much more oil in the reservoir formation than CO_2 flooding did.

Traditionally, the CO_2 Huff-n-Puff technique is considered an effective technique, and field tests have revealed that this technology is generally economically feasible in diverse reservoir environments [6–9]. The governing mechanisms of this technology are as follows: a fraction of the injected CO_2 will be dissolved in the water phase, which increases the water viscosity by 20–30% and its mobility 2-3 times. The CO_2 dissolved in oil decreases the interfacial tension (IFT) in the oil-water contact, and the CO_2 dissolved in oil reduces the oil viscosity 1.5–2.5 times. Also, the CO_2 dissolved in oil increases the oil volume [10]. The dissolution of CO_2 in the oil phase can also increase the total volume of oil and the vaporization of lighter hydrocarbon components [11–15]. Martinez et al. [16] investigated the use of CO_2 as an EOR solvent for heavy oil. Due to multicontact miscibility, the Huff-n-Puff simulation cases also indicate increased oil recovery and reduced matrix oil saturation by CO_2 compared to N_2 injection.

Although the CO_2 Huff-n-Puff process has been determined to be able to improve oil recovery, some negative impacts associated with the application of this technique have been reported. For example, some negative impacts are the reduction of CO_2 concentration, coagulation, and sedimentation of asphaltene in the oil phase due to change in the thermobaric conditions; well and oil field equipment corrosion; and issues with CO_2 transportation [10]. Thus, a considerable effort has been undertaken to develop this technology (in particular, the in situ generated CO_2 technique). This technique involves the injection of underground water into a formation to allow injected chemicals to react with formation materials to release CO_2 inside the reservoir [3]. The advantage of this technique is the elimination of any surface facility and associated negative impacts on the environment. In addition, chemical enhanced oil recovery has recently focused on using surfactants to change oil-wet wettability into water-wet wettability to enhance water imbibition into matrix blocks in the oil reservoirs and to improve the flowing property of crude oil by reducing interfacial surface tension [17–24]. The increase in recovery by CO_2 generation is also attained by maintaining (or increasing) the reservoir pressure, displacing the oil, and eliminating the interface between the oil and CO_2.

Jia et al. [3] conducted a laboratory investigation on in situ CO_2 generation and found that the proposed technology can decrease the injection pressure of the damaged core by 11.7 MPa. Furthermore, the increase rates of the amount of the generated gas and the oil volume escalate with the increase of temperature and system concentration. In addition, the oil volume and the oil viscosity reduction rates increase with the increase of oil viscosity. Under the condition of 60°C, 10 MPa, and 2010 mPa·s, the oil volume increased by 25%, the oil viscosity decreased by 52.7%, and the recovery efficiency improved by 7.6–14.2%.

AlSofi et al. [25] performed a series of surfactant core flooding experiments in carbonate cores under typical reservoir conditions. The core flooding results showed significant oil recovery potential for surfactant flooding (SF) formulations under the investigated conditions. The base SF resulted in a 23.4% incremental recovery after water flooding with a combination of polymer and surfactant. The results also demonstrated the effects of surfactant slug-size and concentration on the recovery performance. Kumar and Mandal [26] found experimentally that alkali-surfactant systems change the wettability of an intermediate-wet quartz rock to water-wet and the change of wettability from oil-wet to water-wet increases the oil recovery significantly. The solution of $C_{19}H_{42}BrN$ surfactant in the presence of sodium metaborate changes the contact angle to 8-9°, whereas the solutions of $C_{12}H_{25}NaO_3S$ in the presence of Na_2CO_3 change the contact angle to 4°. An effective mobility ratio and a reduced IFT between the residual oil and displacing fluid are obtained by the formed emulsion, which is recognized as a potential efficient chemical EOR process. $C_{12}H_{25}NaO_3S$ also forms good emulsions in the presence or absence of alkali, which have good stability compared to other surfactants. Unlike nonionic surfactants, ionic surfactant molecules contain charge and form a charged monolayer at the interface: hence, it is found to be comparatively more capable of reducing the interfacial tension.

Our literature review concludes that the in situ generated CO_2 Huff-n-Puff process with chemical compound surfactant could substantially improve oil recovery performance [27, 28]. However, very limited research has been undertaken in this area, especially for the parametric analysis of the key operating variables for the improvement of oil recovery. Therefore, we performed a numerical simulation and optimization study on the effect of the in situ generated CO_2 compound surfactant Huff-n-Puff method on oil recovery performance for a low permeability fault-block reservoir located in southeast China. The objective of this paper is to examine the important parameters, best practices, and lessons learned that contribute to the success of the in situ generated CO_2 Huff-n-Puff process with compound surfactant. Based on these successes, the optimal operating parameters are analyzed and identified, and recommendations to improve related Huff-n-Puff projects further are presented.

2. Experimental

2.1. In Situ Generated CO_2

2.1.1. Materials. The N_2 gas (purity 99.99%) was supplied by Chengdu Dongfang Electric Gas Co., Ltd. The $NaHCO_3$ and Na_2CO_3 salts were supplied by Sinopharm Chemical Reagent Co., Ltd., were of analytical grade with a purity of >99%, and are shown in Table 1. The specific details of the compound acid made up of CH_3COOH and HCl are also shown in Table 1. Distilled water was used to prepare the solutions.

2.1.2. Apparatus and Procedures. The auxiliary laboratory equipment was purchased from Chengdu Kelong Chemical Reagent Co., Ltd. and included test tubes, stopwatch, sophisticated electronic balance, rubber tubes, glass tubes, and acid burettes. The main apparatus consisted of a reaction vessel (Taixing Xingjian Chemical and Machinery Plant), a high pressure manual metering pump (Jiangsu Huaan Scientific Instruments Co., Ltd.), and a N_2 gas cylinder (Chengdu

Table 1: Source and purity of the reagents used.

Compounds	CAS number	Source	Molar mass (g/mol)	Purity (mass fraction)
N_2	7727-37-9	Chengdu Dongfang Electric Gas Co., Ltd.	28.013	0.9999
$NaHCO_3$	144-55-8	Sinopharm Chemical Reagent Co., Ltd.	84.01	0.999
Na_2CO_3	497-19-8	Sinopharm Chemical Reagent Co., Ltd.	105.99	0.999
CH_3COOH	64-19-7	Sinopharm Chemical Reagent Co., Ltd.	60.05	0.99
HCl	7647-01-0	Sinopharm Chemical Reagent Co., Ltd.	36.46	37.0
$C_{12}H_{25}NaO_3S$	2386-53-0	Chengdu Kelong Chemical Reagent Co., Ltd.	272.38	0.99
$C_{18}H_{29}NaO_3S$	25155-30-0	Chengdu Kelong Chemical Reagent Co., Ltd.	348.48	0.99

Dongfang Electric Gas Co., Ltd.). The experiments were performed inside the apparatus based on the static approach. A schematic of the experimental setup for in situ generated CO_2 is shown in Figure 1. The temperature of the thermostatic air bath was controlled by a temperature controller.

In this experiment, the reaction vessel and lines were evacuated using a vacuum pump prior to introducing the aqueous solution, which consisted of Na_2CO_3, $NaHCO_3$, and compound acid (HCl + CH_3COOH). The concentration of the $NaHCO_3$ solution was the same as that of the Na_2CO_3 solution (20 wt%). The concentration of compound acid was 12.70%.

The reaction vessel was placed in the air bath, and the temperature in the bath was controlled with an immersed thermocouple by an electric furnace to the desired temperature of 60°C. Initially, the desired amounts of the Na_2CO_3 and $NaHCO_3$ solutions were injected into the reaction vessel. Then the compound acid was injected. Subsequently, N_2 was discharged into the system using the pressure amplifier, and the reaction vessel was controlled to reach the desired pressure of 10.00 MPa.

The aqueous phase in the vessel was stirred using a magnetic stirrer. The stirring of the aqueous phase ensured a homogeneous reaction temperature inside the vessel. The temperature was detected by a thermometer within ±0.1°C scale, and the pressure was monitored by a transducer with a precision of 0.01 MPa. Finally, the pressure and the temperature of the system were recorded.

2.2. Surfactant Flooding

2.2.1. Materials. The oil sample was collected from the fault-block formation of China's northeast region. The compositional analysis of dead oil is presented in Table 4. For all Huff-n-Puff tests, the core was saturated with dead oil, at which viscosity is 155.30 mPa·s and density is 908.50 g/cm^3 at 25°C. In addition to the reagents previously described in the in situ generated CO_2 experiment, we used the surfactants of $C_{12}H_{25}NaO_3S$ and $C_{18}H_{29}NaO_3S$ supplied by Chengdu Kelong Chemical Reagent Co., Ltd., which were of analytical grade with a purity of >99% (see Table 1).

2.2.2. Apparatus and Procedures. A schematic diagram of the surfactant flooding experimental setup used in this study is shown in Figure 2.

A sand pack measuring approximately 50 cm in length and 3.5 cm in diameter was prepared with 80–120 mesh sands in a sleeve. The sand was wet-packed with a pneumatic vibrator and the pack was vibrated for about 20 min. The packed core was then triaxially loaded and subjected to an overburden pressure to seal the assembly. Once the core holder was fully wet-packed, the vibrator continued at a relatively high rate for two hours to ensure a tight sand pack. The core holder was placed in a thermostatic air bath and connected to the fluid injection system and sample collection system. The wet-packed sand pack was flooded with crude oil until irreducible water saturation was achieved. The details of the sand pack are presented in Table 2.

The flood tests were conducted horizontally at an ambient temperature of 60°C. After establishing the above conditions, the sand pack was ready for water flooding as an initial oil recovery process. Water was injected at a constant rate of 1.0 mL/min and was continued to one pore volume. Following the water flooding, the next stage was the process of surfactant flooding (in situ generated CO_2 Huff-n-Puff with compound surfactant). In this primary Huff-n-Puff process, the concentrations of the compound acid, Na_2CO_3, and $NaHCO_3$ were all 0.8 mol/L and the concentration of the surfactant was 0.3%.

The method of slug injection formula was selected and conducted as follows: initially, a surfactant solution slug with a specified size of 0.2 pore volume was injected at a constant rate of 1.0 mL/min. Then, the compound acid and the Na_2CO_3 solution were injected at the rate of 1.0 mL/min. At the same time, the $NaHCO_3$ solution was injected at a constant rate of 1.0 mL/min. Subsequently, we cycled the injection of the compound acid together continually with the Na_2CO_3 solution and $NaHCO_3$ solution until the volume of injection reached the 0.1 pore volume. After a 2 h shut-in period, the oil recovery process was initiated. The back pressure was established at 6 MPa. When the shut-in time reached 2 h, we used a measuring cylinder to collect and record the volumes of effluent from the outlet.

The specific procedures of the secondary and tertiary Huff-n-Puff processes were the same as those of the primary Huff-n-Puff process. The oil recovery rate (E_D) of the three cycles of CO_2 Huff-n-Puff with compound surfactant was calculated using

$$E_D = \frac{\sum V_{oi}}{S_{oi} V_P} \times 100\%, \quad (1)$$

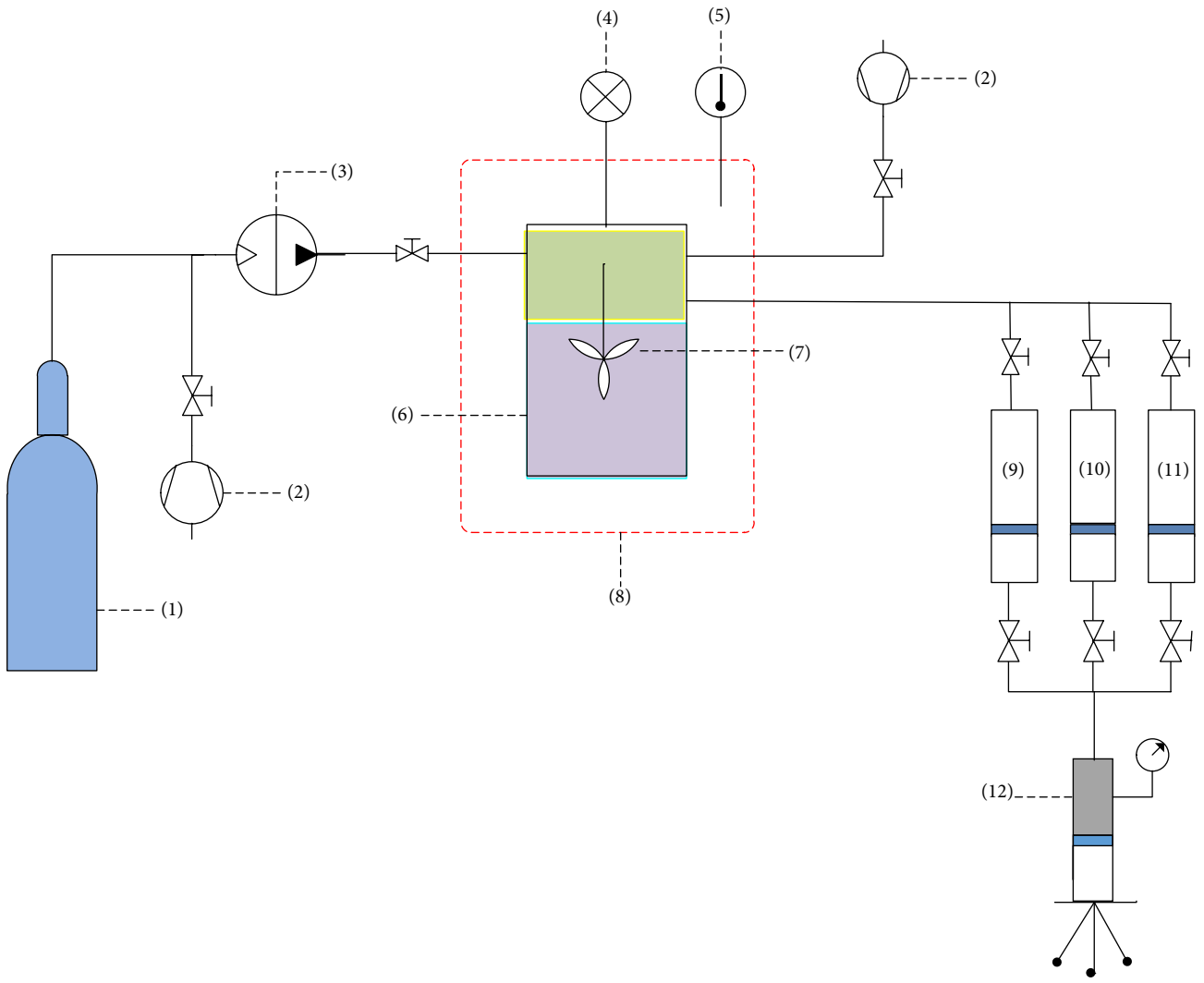

Figure 1: Schematic diagram of the in situ generated CO_2 apparatus. (1) Gas cylinder, (2) vacuum pump, (3) pressure amplifier, (4) pressure gauge, (5) temperature transducer, (6) reaction vessel, (7) magnetic stirrer, (8) thermostatic air bath, (9) Na_2CO_3 solution, (10) $NaHCO_3$ solution, (11) compound acid, and (12) pump.

Table 2: Sand pack filling conditions and properties.

Permeability mD	Porosity (%)	Oil saturation (%)	Water saturation (%)	Temperature (°C)
594.23	39.77	68.87	31.13	60

where V_{oi} is the oil volume collected from outlet, S_{oi} is the original water saturation, and V_P is the pore volume.

3. Numerical Simulation

3.1. Reservoir Modeling Parameters. In this numerical study, a typical low permeability fault-block oil reservoir is taken as an example. A single-well radial plane model was established using STARS™, Ver. 2012, from the Computer Modeling Group (CMG) (Figure 3(a)). Although this process cannot characterize the whole reservoir, the reaction of gas-forming in the formation and change of components can be precisely described. The computational domain contains a total of 14616 active grid blocks ($29 \times 24 \times 21$). In the I direction, from the center of wellbore to the edge, there are three 2 m step grids, ten 5 m ones, and sixteen 9 m ones. In the J direction, a 360° wellbore circle is divided into 24 equal parts with each 15°. In the K direction, the grid is constructed according to the thickness of the real reservoir. The property parameters of porosity, permeability, and thickness are obtained from the well logging data, which are shown in Figures 3(b)–3(d), respectively. The initial oil saturation is about 45%, and the OOIP is about 3.54×10^5 tons. The other reservoir modeling

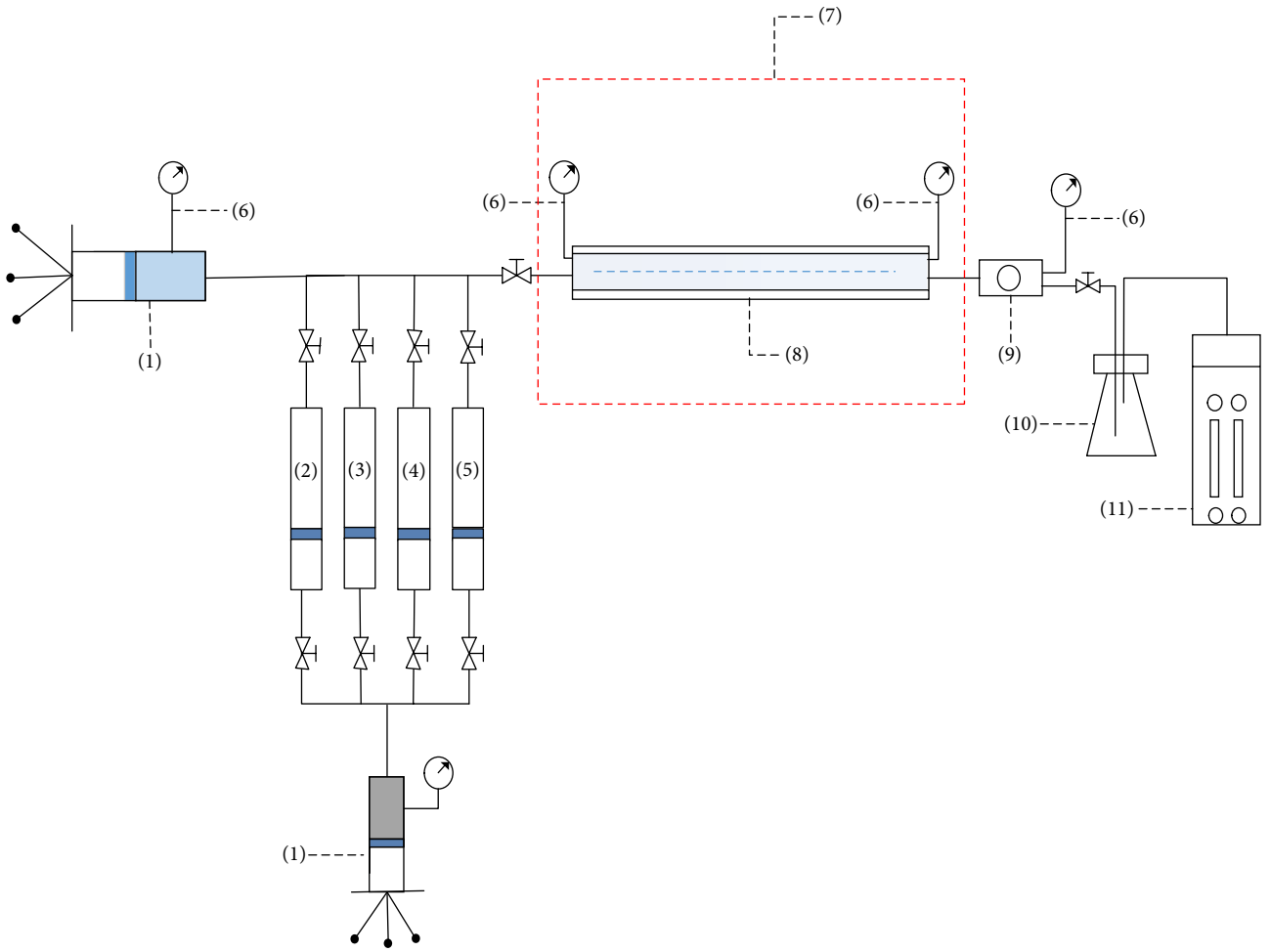

Figure 2: Schematic diagram of the core flooding apparatus. (1) Pump, (2) Na_2CO_3 solution, (3) $NaHCO_3$ solution, (4) acid, (5) compound surfactant, (6) pressure gauge, (7) thermostatic air bath, (8) sand pack tube, (9) back pressure regulator, (10) oil and water collector, and (11) gas meter.

parameters are shown in Table 3. The detailed properties of the sand-rock layer for the oil reservoir are as follows: the volumetric thermal capacity is 2.35×10^6 J/(m^3·°C) and the thermal conductivities are 6.6×10^5 J/(m·d·C) and 8.305×10^3 J/(m·d·C) for the rock and oil samples, respectively.

3.2. Phase Equilibrium and Properties of Fluids. In order to develop PVT thermodynamic equations for the reservoir fluids, the fluids were characterized by analytical tests of constant composition expansion, saturation pressure determination, and single flash tests. The original composition of crude oil is shown in Table 4. Subsequently, the key state parameters for establishing PVT equations were derived from the CMG Winprop™, Ver. 2012, phase behavior simulator. The final results of flash tests and saturation pressure determination fitting are shown in Table 5, and the constant composition expansion results are given in Figure 4. As shown in Table 6, fluid property analysis allowed the lumping of nonaqueous components into five pseudo-components. The mole fractions of each component were CO_2, 2.5%; N_2–C_1, 15.9%; C_2–C_6, 3%; C_7–C_{20}, 30.8%; and C_{21}–C_{32}, 47.8%.

Table 3: Characteristic parameters of the reservoir (at a reservoir temperature of 59°C).

Reservoir depth (m)	1212
Total thickness (m)	97.9
Porosity (%)	5–28
Permeability (mD)	15–90
Drainage radius (m)	200
Original water saturation	0.55
Original formation pressure (MPa)	11.34
Reservoir temperature (°C)	59
Saturation pressure (MPa)	4.25
Viscosity of crude oil (mPa·s)	70.01
Density of crude oil (g/cm^3)	0.8218

3.3. Parameters of In Situ Generated CO_2. The key parameters for the reaction of in situ CO_2 generation in reservoir layers include the gas generation rate, the activation energy, reaction enthalpy, and breakdown temperature [29, 30]. These key reaction parameters can influence the accuracy and reliability

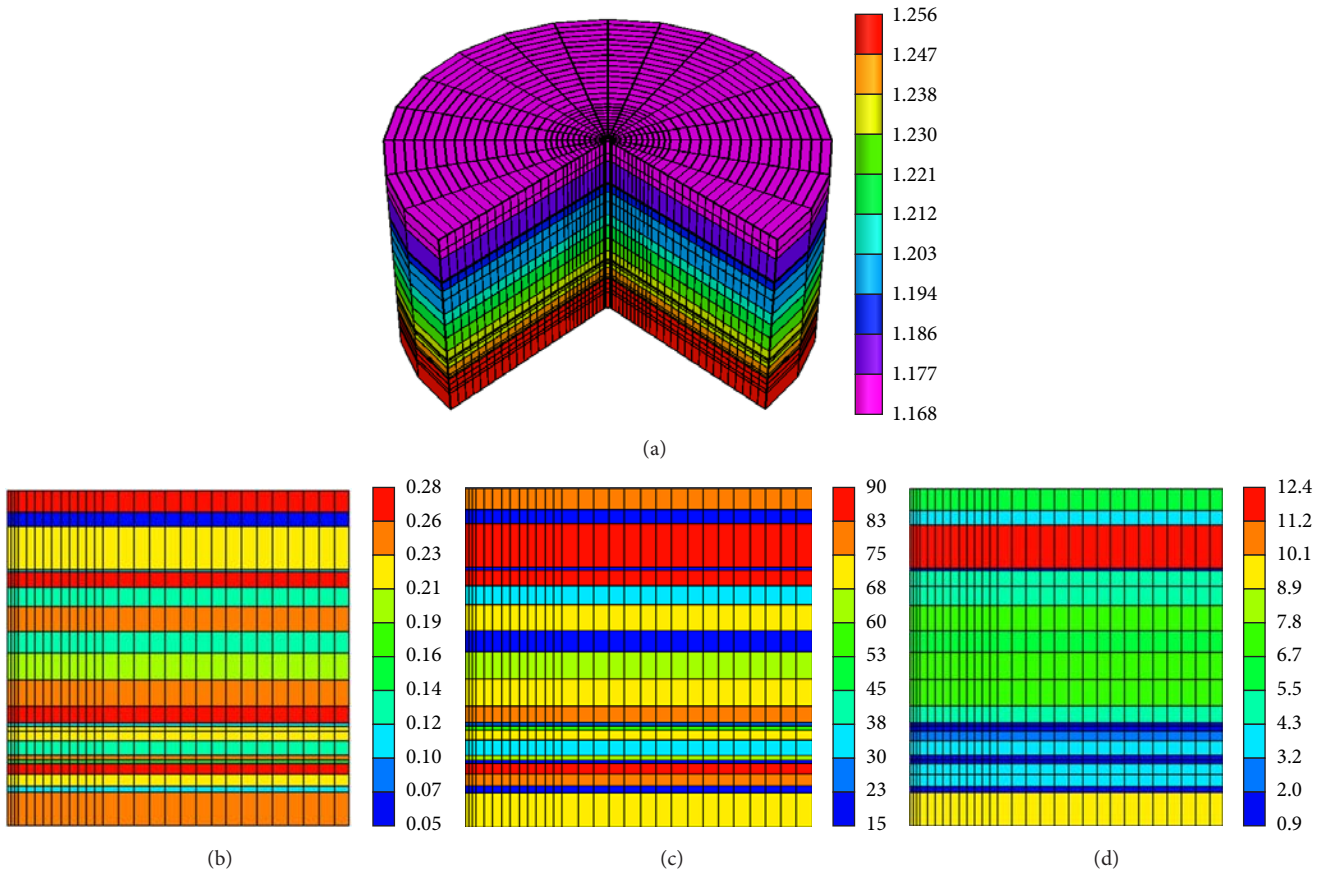

Figure 3: Single-well radial plane model of the southeast oilfield (CMG STARS, Ver. 2012). (a) 3D sectional view of depth, (b) grid porosity, (c) grid permeability (mD), and (d) grid thickness (m).

Table 4: The original composition of crude oil.

Component	CO_2	N_2	C_1	C_2	C_3	iC_4	nC_4	iC_5	nC_5	C_6	C_7	C_8	C_9	C_{10}	C_{11+}
Composition	2.48	0.37	18.02	1.28	0.52	0.24	0.27	0.20	0.15	0.53	0.36	0.27	0.43	0.37	74.51

Table 5: The fitted results of single flash tests and saturation pressure (at a reservoir temperature of 59°C).

Index	Experiment	Simulation	Absolute error	Relative error
Gas oil ratio (m^3/m^3)	16.850	16.610	−0.240	−1.42%
Crude oil density (g/cm^3)	0.909	0.899	−0.01	1.10%
Viscosity (cp)	70.010	70.006	−0.10	−0.002%
Saturation pressure (MPa)	4.250	4.249	−0.001	−0.02%

Table 6: Characteristic parameters of formation of nonaqueous fluid pseudo-components.

Components	Molecular weight (g/mol)	Critical pressure (atm)	Critical temperature (K)	Critical volume (m^3)	Acentric factor —	Coefficient *a* —	Coefficient *b* —
CO_2	44.0100	72.800	304.20	0.0940	0.22500	0.457236	0.077796
N_2 to C_1	16.2863	43.083	189.23	0.0988	0.00865	0.457236	0.077796
C_2 to C_6	50.9499	29.588	394.60	0.2209	0.16607	0.457236	0.077796
C_7 to C_{20}	261.9422	14.612	783.38	0.7529	0.68937	0.457236	0.077796
C_{21} to C_{32}	401.6392	10.786	788.39	1.2247	0.97418	0.365791	0.077796

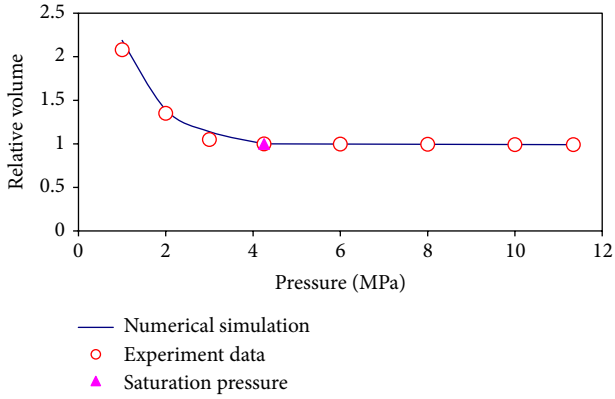

Figure 4: The fitted results of constant composition expansion (at a reservoir temperature of 59°C).

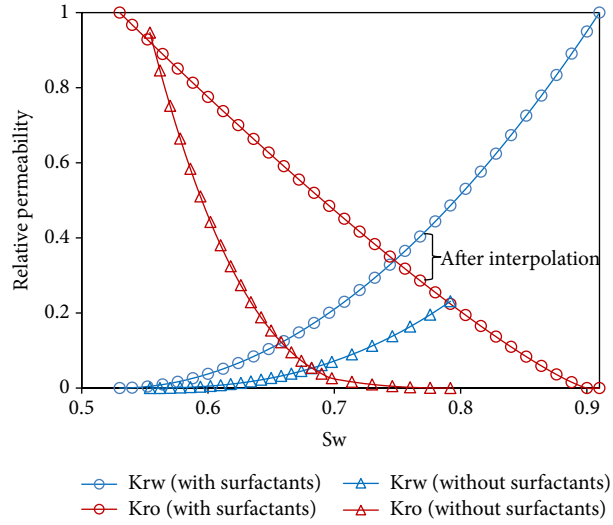

Figure 5: Relative permeability curves (with surfactants, without interpolation).

of the numerical simulation results considerably. The gas generation rate is the reaction rate of CO_2 generation at a given pressure and temperature in the reservoir layers, which is obtained through the experimental results. The activation energy and reaction enthalpy are then calculated based on the established reaction kinetics model and thermodynamic model [31]. According to thermodynamic calculations, the activation energy and the reaction enthalpy are 38150 J/gmol and 45140 J/gmol, respectively.

Typically, two methods are employed for self-generating CO_2 Huff-n-Puff: the single-fluid method and the double-fluid method. In the single-fluid method, a salt solution with low thermal stability is injected into the formation. At the reservoir temperature, the salt will decompose and generate CO_2 and some byproducts. The double-fluid method involves mixing two miscible liquids. Normally, a salt solution and a low-concentration acid solution are mutually injected into the reservoir to react to generate CO_2.

In this paper, we adopt the double-fluid method and define Na_2CO_3 and $NaHCO_3$ as the main reagents because of their simple reaction, low environmental impact, and ease of purchase. The reaction of the reagents occurs with the generation of CO_2 and byproducts as shown in

$$\begin{aligned} &Na_2CO_3 + NaHCO_3 \xrightarrow{H^+} \\ &CO_2 \uparrow + H_2O + NaCl + CH_3COONa \end{aligned} \quad (2)$$

3.4. Parameters of Surfactant Flooding. The primary control parameters of surfactant flooding include oil-water interfacial tension, the relative permeability curves, and the interpolation parameters at low and high interfacial tensions [32–36]. Without the addition of any surfactants, the IFT of the crude oil against its water was measured to be 19.73 mN/m using the axisymmetric drop shape analysis technique [37]. When the surfactants and salts were added to the water, the measured IFTs decreased to 0.96 mN/m. A numerical model for a long core sample was first established to extrapolate key parameters from the lab data. Consequently, the interpolation parameters (used in the relative permeability curve to reflect its trend) at low and high interfacial tensions for the nonwetting phase were determined to be −3.01 and −8.10, respectively, based on the best matching with experimental measurements. With the changes in interpolation parameters, the changing interfacial tensions were reflected in the relative permeability curves (Figure 5).

3.5. Operating Parameters on Key Oil Recovery Performance Indicators. Following the establishment of the proposed model, the total simulation time period for oil recovery was about 12 months. A number of key parameters for the in situ CO_2 generation reaction and surfactant properties were obtained based on curve fitting with the experimental results. Subsequently, simulation studies were conducted to investigate the influences of in situ CO_2 Huff-n-Puff operating parameters on key oil recovery performance indicators, such as the injection volume and mole concentration of the reagent, injection rate, well shut-in time, and oil withdrawal rate. Accordingly, the optimal values of these parameters were obtained by using the single control variable method to quantify the effects of a number of operation parameters. The primary evaluation indexes included the cumulative oil production, incremental oil production, and the oil exchange rate.

4. Results and Discussion

4.1. In Situ Generated CO_2. The analytical model for the gas generation rate was developed based on the experimental data [38]. The corresponding transient pressures and temperatures of the gas self-generation system from model simulations and lab measurements were compared (Figures 6 and 7). Figure 6 shows that the model results have a reasonable agreement with the lab data except for those at the later stages of the reaction with a low system pressure. This is mainly because the generated byproduct is dissolved

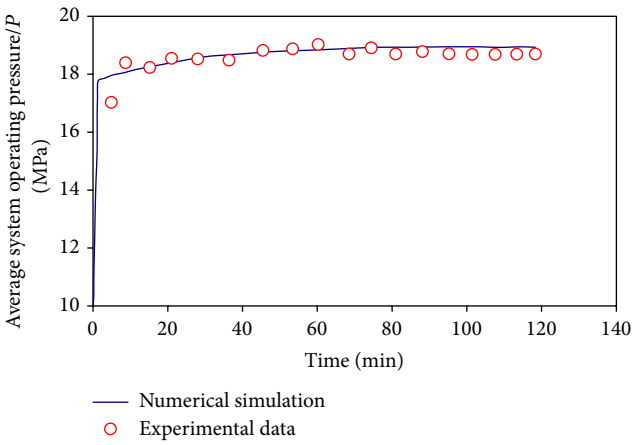

Figure 6: Comparison of the average system operating pressure predicted by the model and the laboratory measurements.

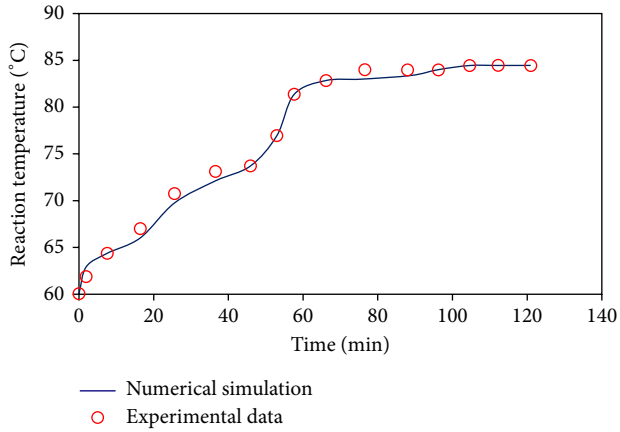

Figure 7: Comparison of the reaction temperature predicted by the model and the laboratory measurements.

in the water, therefore resulting in a lower average system pressure than the model prediction.

In the process of experiment, the pressure increased significantly from an initial 10.00 MPa to 19.03 MPa. This will result in higher effectiveness in exploiting underground oil, because, with the depletion of natural energy, the reservoir pressure will drop lower than a certain value and thus will no longer push the trapped oil toward producing wells. Meanwhile the generated CO_2 gas will increase and maintain the existing pressure in the reservoir.

The temperature of the reaction vessel rose to 84.5°C, an increase of 24.5°C above the original 60.0°C. The exothermic reaction for heat stimulation based on Na_2CO_3, $NaHCO_3$, and the compound acid is unique as the heat generated in the process is used for reducing the viscosity of crude oil. In addition, the byproducts are CO_2, NaCl, H_2O, and CH_3COONa, which are nondamaging to the reservoir.

4.2. Surfactant Flooding. Figure 8 shows the detailed comparison of the oil recovery rate measured from the lab data with that predicted from the numerical model. An excellent

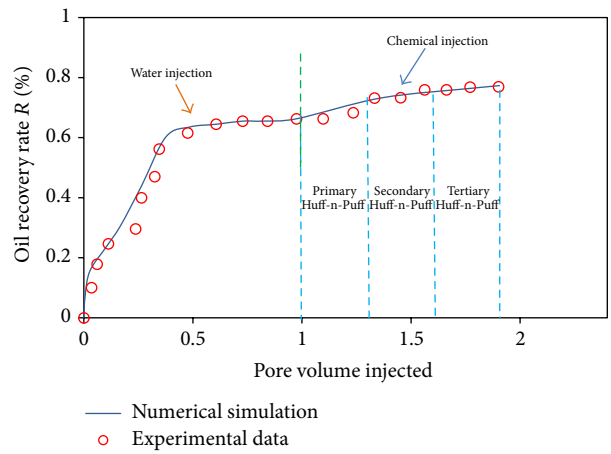

Figure 8: The oil recovery rate of surfactant flooding (at a temperature of 60°C).

agreement is evident between the experimentally measured and numerically simulated profiles with respect to oil recovery rate.

By considering the financial loss caused by surfactant adsorption and the interfacial tension reduction, $C_{18}H_{29}NaO_3S$ was found to be the most appropriate candidate for surfactant flooding among the tested materials [32]. During the lab test, three Huff-n-Puff cycles were performed. The procedure was as follows: the water flooding was first carried out on the long core sample. Next, the reagent solution was mixed with the chemical surfactants. After a certain shut-in period, the oil recovery process was initiated. The overall oil recovery rate increased by 10.69%, in which the primary Huff-n-Puff increased by 6.93%, the secondary Huff-n-Puff increased by 2.71%, and the tertiary Huff-n-Puff increased by 1.05%.

This clear enhancement of oil recovery occurred mainly because, by contacting surfactants and CO_2, the crude oil volume was swollen, its viscosity was decreased, and interfacial tension was reduced. Crude oil is driven by solution gas, as light-components are extracted to the injected CO_2 phase; the mechanisms of solution gas driving and light-components extraction play important roles in recovering oil production [39]. The desirable outcomes achieved in these experiments provided fundamental proof for studying the operating parameters on key oil recovery performance indicators in the next step.

4.3. Effect of Volume and Mole Concentration of Reagent. The reagent injection volume directly affects the quantity of in situ generated CO_2, and the quantity of generated CO_2 further determines the effectiveness of the Huff-n-Puff process on oil recovery. In this analysis, the mole concentration of the reagent was fixed at 5.0%, and seven different injection volumes from 250 t up to 800 t were selected during a fixed time period of 12 months to evaluate the effect of injection volume on oil recovery performances. Figure 9 shows the variation of the cumulative oil production at different injection volumes. It is clear that the cumulative oil production increases with

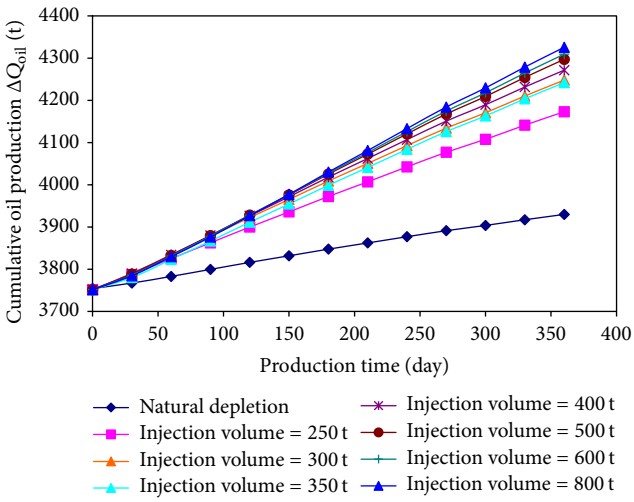

Figure 9: Cumulative oil production at different injection volumes.

the reagent injection volume. The reason for this is that more CO_2 with higher pressure will be generated in the oil-rich layer, and thus more oil is recovered. However, the oil exchange rate (α) would not necessarily follow the same variation trend. α is defined as the ratio of increased oil production during the recovery period (ΔQ_{oil}) to the total injection volume of the reagent (Q_{reag}) as shown in

$$\alpha = \frac{\Delta Q_{oil}}{Q_{reag}}. \quad (3)$$

Figure 10 presents the variations of the increased oil production and the associated α with different injection volumes of the gas reagent. The oil exchange rate first increases with the injection volume to a maximum value of about 1.57 t/t. Next, it decreases with a further increase of the injection volume. This occurs mainly because the increase in the injected reagent volume reduces the relative fraction of the surfactant and thus decreases the effect of the surfactant on alternating the wettability and spontaneous imbibition of water into the oil-containing matrix [40]. This results in lower effectiveness in driving oil out of the matrix. Based on considerations of technical feasibility and economic practice, the optimal injection volume of the reagent should be maintained at around 250 t.

In addition to injection volume, chemical reagent concentration also is a critical parameter governing oil recovery. Typically, to generate sufficient CO_2 in the oil matrix, the solution with a lower concentration of reagent will require a higher injection volume, which in turn would be limited by the capability of the existing field facility. In the case of a higher concentration, the injected less solution tends to be concentrated in the near wellbore area. Therefore, the effective radius of the Huff-n-Puff region will be reduced significantly, and the self-generated CO_2 will not displace the oil from the matrix deep in the toe of the reservoir effectively.

Figures 11 and 12 demonstrate and compare the effect of solution concentration on oil recovery. The reagent mole concentration varies in a relatively large range from 2% to

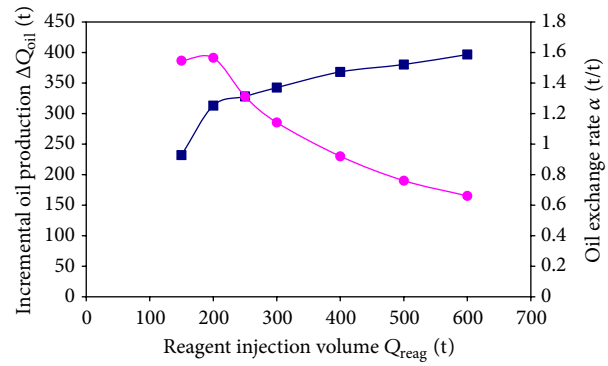

Figure 10: Variations of the incremental oil production and oil exchange rate at different reagent injection volumes.

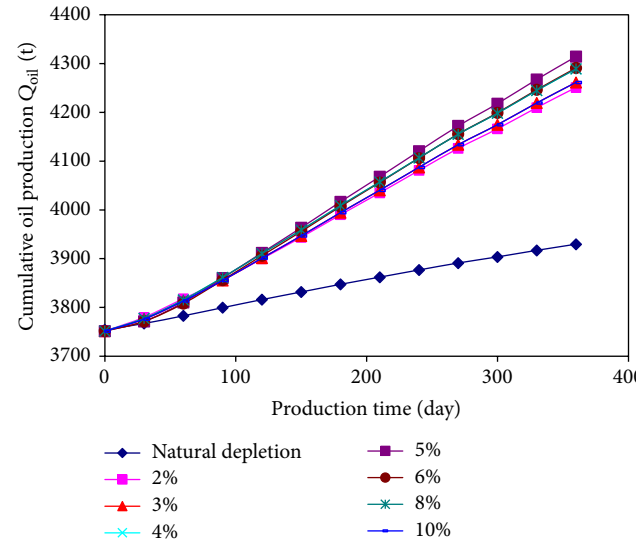

Figure 11: The variation of the cumulative oil production with injected solution at different reagent solution mole concentrations.

10%. As expected, Figure 11 shows that the cumulative oil production first increases with the solution concentration and then decreases with further concentration elevation. The maximum oil production occurs at approximately 5% mole concentration. Figure 12 shows the effect of reagent concentration on the increased oil production and the oil exchange rate. It is clear that both terms reach their maximum at the optimal concentration of about 5%. At higher concentrations, the increased oil production decreases from a peak value of 390 t to about 330 t at the concentration of 10%, while the exchange rate is reduced by almost 16% (i.e., from 1.6 to 1.1).

4.4. Effect of the Injection Rate. The injection rate of the reagent solution is an important operational variable that has a significant impact on the cost, safety, duration, and ultimate success of in situ Huff-n-Puff oil recovery [12, 41]. The reagent solution injection rate directly determines the total mass of reagent available in the oil matrix to generate CO_2 throughout the overall duration of chemical injection. Additionally, the reagent injection rate can effectively impact the rate of

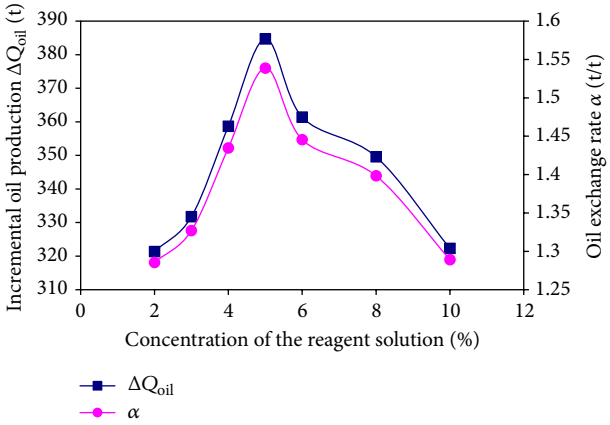

Figure 12: Variations of the incremental oil production and oil exchange rate at different reagent solution mole concentrations.

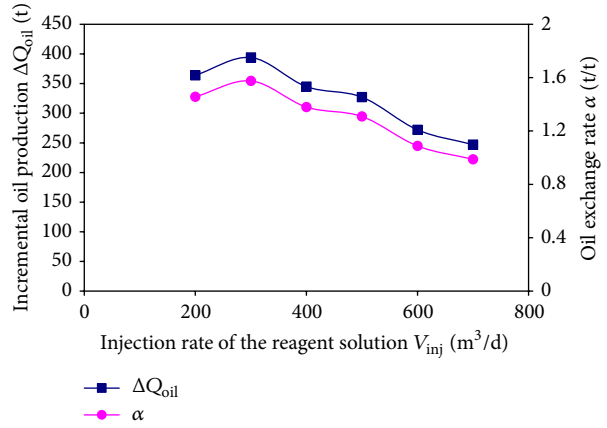

Figure 13: The incremental oil production and oil exchange rate at different reagent solution injection rates.

the generation of CO_2 bubbles in the vicinity of the injector. Figure 13 shows the effect of different injection rates (V_{inj}) on the increased oil production and the oil exchange rate considering a fixed injection amount of about 250 t. As V_{inj} increases from 300 to 700 m^3/d, the reduced oil production is about 150 t in total and the oil exchange rate considerably decreases from 1.5 to 1.0 (a reduction of approximately 33%). This observation indicates that the injection rate of the reagent solution can substantially affect Huff-n-Puff oil recovery compared with parameters. However, it is not often operationally feasible to inject reagent solution at a high rate due to operational limits on the injection pressure (and hence the injection rate) to avoid matrix fracture or well blowout. Therefore, considering the feasibility and existing capability of the oil well, the optimal injection rate of interest in this study is recommended to be about 300 m^3/d.

4.5. Effect of Well Shut-In Time. The shut-in time is another important operating factor for the oil recovery performance. Typically, a certain reaction time is required for the generated CO_2 to diffuse so that it will be fully dissolved in the crude

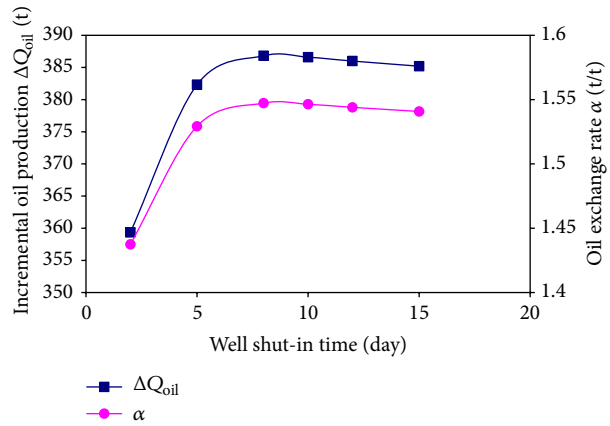

Figure 14: The incremental oil production and oil exchange rates at different well shut-in time periods.

oil within the matrix. This is because a certain time period is required for the diffusion and spread of the in situ generated CO_2 through the low permeability layer. Therefore, the well should be shut in for a certain time period. During this period, pressure dissipation and fluid diffusion dominate the fluid flow process behind the flood front, leading to more efficient displacement of the hydrocarbon by the CO_2 Huff-n-Puff approach. However, if an extended shut-in time is applied [42], the long soaking period causes the in situ generated CO_2 to spread into the deep layer of the formation boundary of the oil well, weakening the elastic driving energy and reducing the miscible condition of the CO_2 with the oil in the main recovery region.

Figure 14 illustrates the effects of different well shut-in times (from 2 to 15 d) between two consecutive recovery cycles on the performance of Huff-n-Puff oil recovery. Both the incremental oil production and the oil exchange rate clearly increase with a shut-in period of up to 8 d. They start to decrease after a longer period because of the excessive diffusion of CO_2 towards the formation boundaries of the oil well. Considering the practical operating feasibility, the optimal shut-in time for effective Huff-n-Puff oil recovery is recommended to be around 8 d.

4.6. Effect of the Oil Withdrawal Rate. Figure 15 shows the variation in Huff-n-Puff oil recovery with different oil withdrawal rates. As withdrawal increases, the incremental oil production and the exchange rate initially increase significantly, but they eventually reach their asymptotes when the withdrawal rate exceeds 7 m^3/d. This occurs mainly because the excessive withdrawal rate causes a considerable depression of the CO_2 pressure within the formation layer and consequently lowers the oil displacement effect from the in situ generated CO_2. Based on this analysis, the practical oil withdrawal rate in the context of this study is recommended to be around 7 m^3/d.

4.7. Comparison of Different Exploitation Modes. Several critical operating variables for Huff-n-Puff CO_2 oil recovery

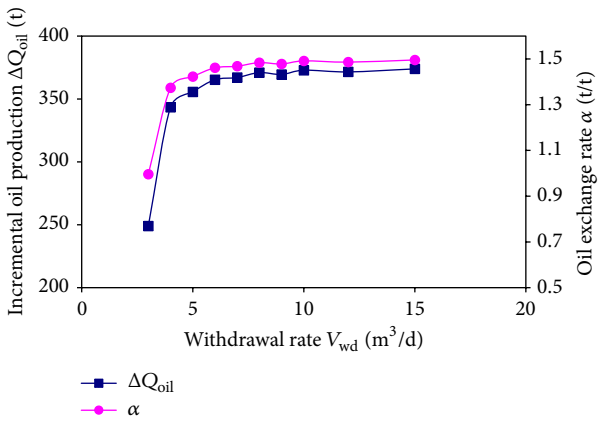

FIGURE 15: The incremental oil production and oil exchange rate at different oil withdrawal rates.

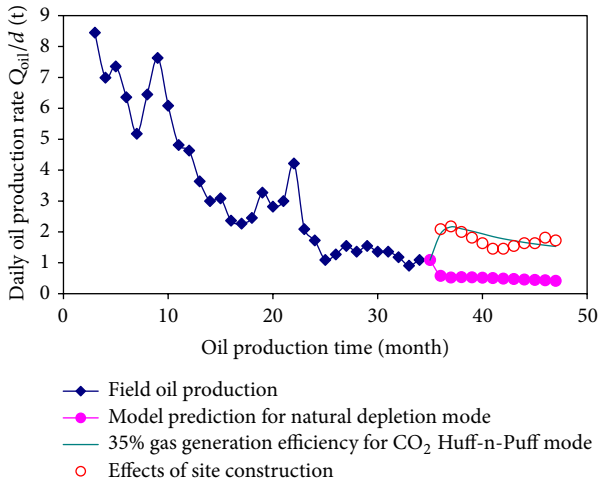

FIGURE 16: The daily oil production rate in different recovery modes.

were identified based on the above comprehensive parametric analysis. Therefore, for the oil well studied in this case, the benefits of in situ generated CO_2 Huff-n-Puff on the oil production are now evaluated. Based on the results of the reaction efficiency of gas generation in the underground, the value of actual reaction efficiency is equal to 35% of the theoretical value. Thus, the gas generation efficiency of the model is now amended by 35% of the theoretical value to provide an accurate prediction. Figures 16 and 17 compare the cumulative and daily oil production under a natural depletion scenario with those in the Huff-n-Puff recovery process. For the Huff-n-Puff process, the operating parameters include the injection volume of reagent 250 t, the mole concentration of 5.0%, the injection rate of 300 m^3/d, and the well shut-in time of 8 d. Figure 16 shows that, in the natural depletion scenario, the daily oil production rate decreases with the production time. Since the onset of the 35th month, the Huff-n-Puff recovery mode is initiated with the injection of a reagent to generate high pressure CO_2 within the oil layer. The corresponding production rate is boosted instantaneously up to 2.2 t/d, and then the rate gradually declines over the course

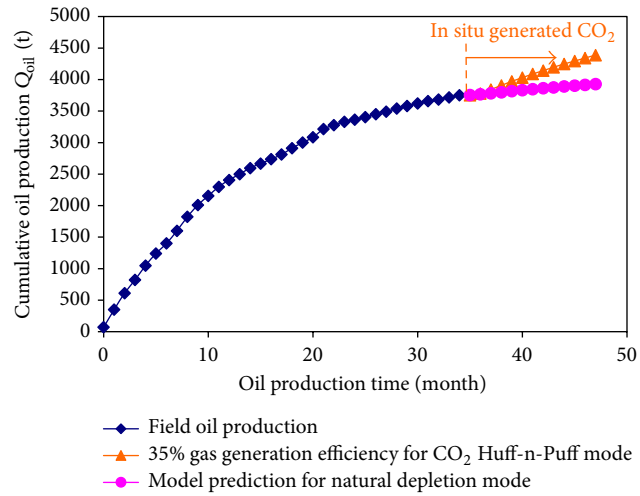

FIGURE 17: The cumulative oil production in different recovery modes.

of the remainder of the recovery process. Overall, the daily production rate is increased by more than 100% relative to the production at the end period of the natural depletion mode. Consequently, Figure 17 shows that the incremental oil production during the 12-month time period is about 610 t in the Huff-n-Puff recovery mode, which is almost 3.7 times higher than the incremental oil production in the natural depletion mode. Therefore, we conclude that, in this region, substantial oil production increase is achieved by the in situ generated CO_2 compound surfactant Huff-n-Puff method.

5. Conclusions

(i) The in situ generated CO_2 Huff-n-Puff method with compound surfactant is a new technology to enhance oil recovery in a low permeability fault-block reservoir. This method mitigates a number of negative impacts of external CO_2 injection on the environment, the lack of field equipment reliability, cost issues, well corrosion, and the transportation of CO_2.

(ii) In the numerical model, the key parameters of reaction and surfactant flooding are experimentally determined. The laboratory results agree with the simulated results for the daily production rate in the period of Huff-n-Puff.

(iii) The results indicate that (a) the injection volume and mole concentration of the reagent and the oil fluid withdrawal rate have important effects compared with other parameters and (b) optimal values exist to maximize the incremental oil production. We found that, for the low permeability fault-block reservoir studied in this paper, the optimal range of these operating parameters is 250 t for the injection volume; 5% for the mole concentration of the reagent; 7 m^3/d for the oil fluid withdrawal rate; 300 m^3/d for the injection rate of the reagent; and 8 d for the well shut-in time.

Competing Interests

The authors declare that they have no competing interests.

Acknowledgments

This work was supported by the National Science Foundation of China (no. 51274173) and the Sichuan Provincial Innovation Team (no. 16TD0010).

References

[1] E. Manrique, C. Thomas, R. Ravikiran et al., "EOR: current status and opportunities," in *Proceedings of the SPE Improved Oil Recovery Symposium*, SPE-130113-MS, Tulsa, Okla, USA, April 2010.

[2] J. J. Sheng, "Status of surfactant EOR technology," *Petroleum*, vol. 1, no. 2, pp. 97–105, 2015.

[3] X. Jia, K. Ma, Y. Liu, B. Liu, J. Zhang, and Y. Li, "Enhance heavy oil recovery by in-situ carbon dioxide generation and application in China offshore oilfield," in *Proceedings of the SPE Enhanced Oil Recovery Conference*, pp. 68–73, Kuala Lumpur, Malaysia, July 2013.

[4] A. Bera and T. Babadagli, "Relative permeability of foamy oil for different types of dissolved gases," *SPE Reservoir Evaluation & Engineering*, 2016.

[5] D. Olsen, "CO_2 EOR production properties of chalk," in *Proceedings of the SPE EUROPEC/EAGE Annual Conference and Exhibition*, SPE, Vienna, Austria, May 2011.

[6] W. Wan and S. Wang, "Determination of residual oil saturation and connectivity between injector and producer using interwell tracer tests," *Journal of Petroleum Engineering & Technology*, vol. 3, no. 3, pp. 18–24, 2013.

[7] J. Ma, X. Wang, R. Gao et al., "Enhanced light oil recovery from tight formations through CO_2 huff 'n' puff processes," *Fuel*, vol. 154, pp. 35–44, 2015.

[8] A. Q. Firouz and F. Torabi, "Utilization of carbon dioxide and methane in huff-and-puff injection scheme to improve heavy oil recovery," *Fuel*, vol. 117, no. 2, pp. 966–973, 2014.

[9] D. S. Rivera, K. Mohanty, and M. Balhoff, "Reservoir simulation and optimization of Huff-and-Puff operations in the Bakken Shale," *Fuel*, vol. 147, pp. 82–94, 2015.

[10] K. K. Gutnersky, A. K. Shakhverdiev, and Y. G. Mamedov, "In-situ generation of carbon dioxide: new way to increase oil recovery," in *Proceedings of the SPE European Petroleum Conference*, SPE-65170-MS, Paris, France, October 2000.

[11] F. Torabi, A. Q. Firouz, A. Kavousi, and K. Asghari, "Comparative evaluation of immiscible, near miscible and miscible CO_2 huff-n-puff to enhance oil recovery from a single matrix-fracture system (experimental and simulation studies)," *Fuel*, vol. 93, pp. 443–453, 2012.

[12] Z. Li and Y. Gu, "Soaking effect on miscible CO_2 flooding in a tight sandstone formation," *Fuel*, vol. 134, no. 9, pp. 659–668, 2014.

[13] F. Torabi and K. Asghari, "Effect of operating pressure, matrix permeability and connate water saturation on performance of CO_2 huff-and-puff process in matrix-fracture experimental model," *Fuel*, vol. 89, no. 10, pp. 2985–2990, 2010.

[14] F. Yang, J. Deng, and Y. Xue, "Jiangsu oil field carbon dioxide cyclic stimulation operations: lessons learned and experiences gained," in *Proceedings of the SPE International Conference on CO2 Capture, Storage, and Utilization*, New Orleans, La, USA, November 2010.

[15] C. Chen, M. Balhoff, and K. K. Mohanty, "Effect of reservoir heterogeneity on improved shale oil recovery by CO_2 huff-n-puff," in *Proceedings of the SPE Unconventional Resources Conference*, pp. 410–425, April 2012.

[16] J. N. F. Martinez, M. Abbaszadeh, R. P. Olguin, E. P. Martinez, and A. R. Figueroa, "Evaluation of CO2-EOR gas injection in a heavy-oil naturally fractured reservoir," in *Proceedings of the SPE Heavy and Extra Heavy Oil Conference*, SPE-171054-MS, Medellín, Colombia, September 2014.

[17] J. J. Sheng, "Comparison of the effects of wettability alteration and IFT reduction on oil recovery in carbonate reservoirs," *Asia-Pacific Journal of Chemical Engineering*, vol. 8, no. 1, pp. 154–161, 2013.

[18] K. Rai, R. T. Johns, M. Delshad, L. W. Lake, and A. Goudarzi, "Oil-recovery predictions for surfactant polymer flooding," *Journal of Petroleum Science and Engineering*, vol. 112, pp. 341–350, 2013.

[19] J. J. Sheng, "Review of surfactant enhanced oil recovery in carbonate reservoirs," *Advances in Petroleum Exploration and Development*, vol. 6, no. 1, pp. 1–10, 2013.

[20] W. Wan, A. Raj, T.-P. Hsu, P. Lohateeraparp, J. H. Harwell, and B.-J. B. Shiau, "Designing surfactant-only formulations for a high salinity and tight reservoir," *International News on Fats, Oils and Related Materials*, vol. 24, no. 10, pp. 622–627, 2013.

[21] A. A. Dehghan, M. Masihi, and S. Ayatollahi, "Phase behavior and interfacial tension evaluation of a newly designed surfactant on heavy oil displacement efficiency; effects of salinity, wettability, and capillary pressure," *Fluid Phase Equilibria*, vol. 396, pp. 20–27, 2015.

[22] K. Babu, N. Pal, A. Bera, V. K. Saxena, and A. Mandal, "Studies on interfacial tension and contact angle of synthesized surfactant and polymeric from castor oil for enhanced oil recovery," *Applied Surface Science*, vol. 353, pp. 1126–1136, 2015.

[23] H. Pei, G. Zhang, J. Ge, L. Jin, and L. Ding, "Study on the variation of dynamic interfacial tension in the process of alkaline flooding for heavy oil," *Fuel*, vol. 104, pp. 372–378, 2013.

[24] M. M. F. Hasan, E. L. First, F. Boukouvala, and C. A. Floudas, "A multi-scale framework for CO_2 capture, utilization, and sequestration: CCUS and CCU," *Computers and Chemical Engineering*, vol. 81, no. 8, pp. 2–21, 2015.

[25] A. M. AlSofi, J. S. Liu, M. Han, and S. Aramco, "Numerical simulation of surfactant–polymer coreflooding experiments for carbonates," *Journal of Petroleum Science and Engineering*, vol. 111, no. 11, pp. 184–196, 2013.

[26] S. Kumar and A. Mandal, "Studies on interfacial behavior and wettability change phenomena by ionic and nonionic surfactants in presence of alkalis and salt for enhanced oil recovery," *Applied Surface Science*, vol. 372, pp. 42–51, 2016.

[27] Q. Liu, M. Dong, S. Ma, and Y. Tu, "Surfactant enhanced alkaline flooding for Western Canadian heavy oil recovery," *Colloids and Surfaces A: Physicochemical and Engineering Aspects*, vol. 293, no. 1–3, pp. 63–71, 2007.

[28] V. Mirchi, S. Saraji, L. Goual, and M. Piri, "Dynamic interfacial tension and wettability of shale in the presence of surfactants at reservoir conditions," *Fuel*, vol. 148, pp. 127–138, 2015.

[29] B. Y. Jamaloei, R. Kharrat, and F. Torabi, "A mechanistic analysis of viscous fingering in low-tension polymer flooding in heavy-oil reservoirs," *Journal of Petroleum Science and Engineering*, vol. 78, no. 2, pp. 228–232, 2011.

[30] S. Carroll, Y. Hao, M. Smith, and Y. Sholokhova, "Development of scaling parameters to describe CO_2—rock interactions within Weyburn-Midale carbonate flow units," *International Journal of Greenhouse Gas Control*, vol. 16, pp. S185–S193, 2013.

[31] B. J. B. Shiau, T.-P. Hsu, B. L. Roberts, and J. H. Harwell, "Improved chemical flood efficiency by in situ CO_2 generation," in *Proceedings of the 17th SPE Improved Oil Recovery Symposium (IOR '10)*, pp. 1077–1086, Tulsa, Okla, USA, April 2010.

[32] S. Park, E. S. Lee, and W. R. W. Sulaiman, "Adsorption behaviors of surfactants for chemical flooding in enhanced oil recovery," *Journal of Industrial and Engineering Chemistry*, vol. 21, no. 1, pp. 1239–1245, 2015.

[33] W. Hongyan, C. Xulong, Z. Jichao, and Z. Aimei, "Development and application of dilute surfactant-polymer flooding system for Shengli oilfield," *Journal of Petroleum Science and Engineering*, vol. 65, no. 1-2, pp. 45–50, 2009.

[34] A. Mehranfar and M. H. Ghazanfari, "Investigation of the microscopic displacement mechanisms and macroscopic behavior of alkaline flooding at different wettability conditions in shaly glass micromodels," *Journal of Petroleum Science and Engineering*, vol. 122, pp. 595–615, 2014.

[35] L. Chen, G. Zhang, J. Ge, P. Jiang, J. Tang, and Y. Liu, "Research of the heavy oil displacement mechanism by using alkaline/surfactant flooding system," *Colloids and Surfaces A: Physicochemical and Engineering Aspects*, vol. 434, no. 19, pp. 63–71, 2013.

[36] Y. Zhu, Q. Hou, G. Jian, D. Ma, and Z. Wang, "Current development and application of chemical combination flooding technique," *Petroleum Exploration and Development*, vol. 40, no. 1, pp. 96–103, 2013.

[37] P. Cheng, D. Li, L. Boruvka, Y. Rotenberg, and A. W. Neumann, "Automation of axisymmetric drop shape analysis for measurements of interfacial tensions and contact angles," *Colloids and Surfaces*, vol. 43, no. 2, pp. 151–167, 1990.

[38] F. Yang, J. Deng, and W. Zhu, "Lab experimental study on in-situ carbon dioxide generation to enhance oil recovery," *Complex Hydrocarbon Reservoirs*, vol. 5, no. 4, pp. 70–72, 2012.

[39] C. Song and D. Yang, *Performance Evaluation of CO_2 Huff-n-Puff Processes in Tight Oil Formations*, Society of Petroleum Engineers, 2013.

[40] P. Bikkina, J. Wan, Y. Kim, T. J. Kneafsey, and T. K. Tokunaga, "Influence of wettability and permeability heterogeneity on miscible CO_2 flooding efficiency," *Fuel*, vol. 166, pp. 219–226, 2015.

[41] R. Safi, R. K. Agarwal, and S. Banerjee, "Numerical simulation and optimization of CO_2 utilization for enhanced oil recovery from depleted reservoirs," *Chemical Engineering Science*, vol. 144, pp. 30–38, 2016.

[42] J. Ma, X. Wang, R. Gao et al., "Study of cyclic CO_2 injection for low-pressure light oil recovery under reservoir conditions," *Fuel*, vol. 174, pp. 296–306, 2016.